

Long-term growth of the Himalaya inferred from interseismic InSAR measurement

Raphaël Grandin¹, Marie-Pierre Doin¹, Laurent Bollinger², Béatrice Pinel-Puysségur², Gabriel Ducret¹, Romain Jolivet³, and Soma Nath Sapkota⁴

¹Ecole Normale Supérieure, UMR 8538, F-75231 Paris, France

²CEA, DAM, DIF, F-91297 Arpajon, France

³Institut des Sciences de la Terre, UMR 5275, F-38041 Grenoble, France

⁴Department of Mines and Geology, National Seismological Centre, Lainchaur, Kathmandu, Nepal

ABSTRACT

The rise and support of the ~5000 m topographic scarp at the front of Indian-Eurasian collision in the Himalaya involves long-term uplift above a mid-crustal ramp within the Main Himalayan Thrust (MHT) system. Locking of the shallower portion of the flat-ramp-flat during the interseismic period also produces transient uplift above the transition zone. However, spatial and temporal relationships between permanent and transient vertical deformation in the Himalaya are poorly constrained, leading to an unresolved causal relationship between the two. Here, we use interferometric synthetic aperture radar (InSAR) to measure interseismic uplift on a transect crossing the whole Himalaya in central Nepal. The uplift velocity of 7 mm/yr at the front of the Annapurna mountain range is explained by an 18–21 mm/yr slip rate on the deep shallow-dipping portion of the MHT, with full locking of the mid-crustal ramp underlying the High Himalaya. The transient uplift peak observed by InSAR matches spatially with the long-term uplift peak deduced from the study of trans-Himalayan river incision, although models of the seismic cycle involving thrusting over a ramp of fixed geometry predict an ~20 km separation between the two peaks. We argue that this coincidence indicates that today's mid-crustal ramp in central Nepal is located southward with respect to its average long-term location, suggesting that mountain growth proceeds by frontward migration of the ramp driven by underplating of material from the Indian plate under the Himalaya.

INTRODUCTION

Active thrusting of India under the Tibetan Plateau gives rise to great earthquakes that rupture the interseismically locked superficial portion of the Main Himalayan Thrust (MHT) system (Fig. 1). In Nepal, uplifted Holocene terraces on the hanging wall of the Main Fron-

tal Thrust (MFT)—the southernmost branch of the MHT system—indicate that nearly the whole 20 mm/yr convergence rate across the Himalaya is accommodated by the MFT (Lavé and Avouac, 2001). Yet, the most prominent topographic step associated with the continental collision, often called the physiographic tran-

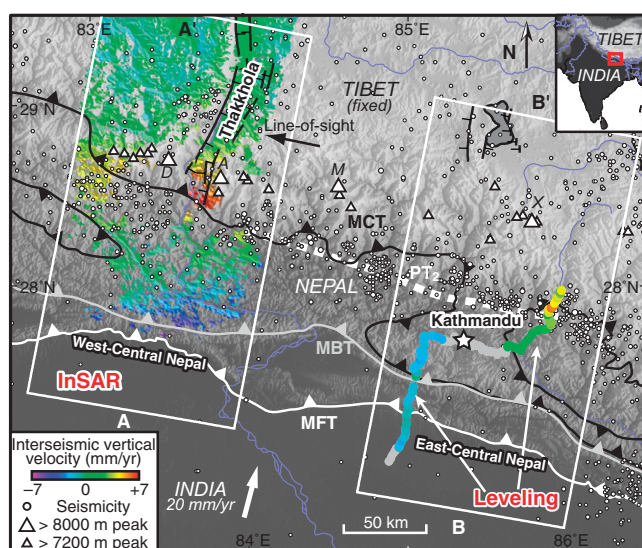
sition 2 (PT₂), is located ~100 km north of the MFT, at the front of the High Himalaya (Fig. 1). There, steep topographic slopes coincide with a secondary local maximum in the bimodal long-term uplift profile (Fig. 2). These features have been explained by the flat-ramp-flat geometry of the MHT, with the localized zone of uplift in the hinterland marking the presence of an underlying mid-crustal ramp (e.g., Cattin and Avouac, 2000). Another interpretation for locally enhanced exhumation rates ~100 km north of the MFT relies on out-of-sequence activation of a new fault partly coinciding with the Main Central Thrust (MCT)—the northernmost branch of the MHT system—with the possible additional contribution of intense rainfall along the orographic barrier (e.g., Hodges et al., 2004; Wobus et al., 2005).

During the interseismic period, the shallowest portion of the MHT is locked. Constraining the location of the locking boundary within the MHT should permit us to pinpoint which updip portion of the MHT contributes most to long-term uplift in the Himalaya: a steep fault emerging near the MCT or the ramp-flat connection to the MFT. Resolving this question could help to identify the most probable scenario among these two radically different views on the evolution of the Himalayan orogeny.

INSAR MEASUREMENT OF SURFACE VELOCITY FIELD

Using satellite-borne interferometric synthetic aperture radar (InSAR), we map the interseismic velocity field across the Himalaya. In this region, the poor coherence is the primary obstacle to InSAR measurements. To tackle this issue, we apply a series of corrections that improve the spatial coherence of wrapped interferograms (see the GSA Data Repository¹). We use 29 C-band SAR images acquired between 2003 and 2010 over west-central Nepal. The images are precisely coregistered with respect to a single master image, and interferograms are computed using an *a priori* knowledge of

Figure 1. Vertical interseismic uplift in central Nepal. Map of central Nepal showing the main faults related to shortening across the Himalaya. MCT—Main Central Thrust; MBT—Main Boundary Thrust; MFT—Main Frontal Thrust. The three branches merge at depth with the Main Himalayan Thrust dipping north under Tibet. Interferometric synthetic aperture radar (InSAR) and leveling (Jackson and Bilham, 1994) measurements of the vertical velocity are color coded from blue (subsidence) to red (uplift). Profiles A–A' and B–B' are shown in Figure 2. White circles represent the microseismic activity between 2000 and 2008 recorded by the National Seismological Centre of Nepal. Small and large white triangles indicate the locations of the peaks with elevation above 7200 m and 8000 m, respectively (A—Annapurna; D—Dhaulagiri; M—Manaslu; X—Xishapangma). PT₂—physiographic transition 2 (from Wobus et al., 2005).



¹GSA Data Repository item 2012309, details of the InSAR processing scheme and inversion procedure, is available online at www.geosociety.org/pubs/ft2012.htm, or on request from editing@geosociety.org or Documents Secretary, GSA, P.O. Box 9140, Boulder, CO 80301, USA.

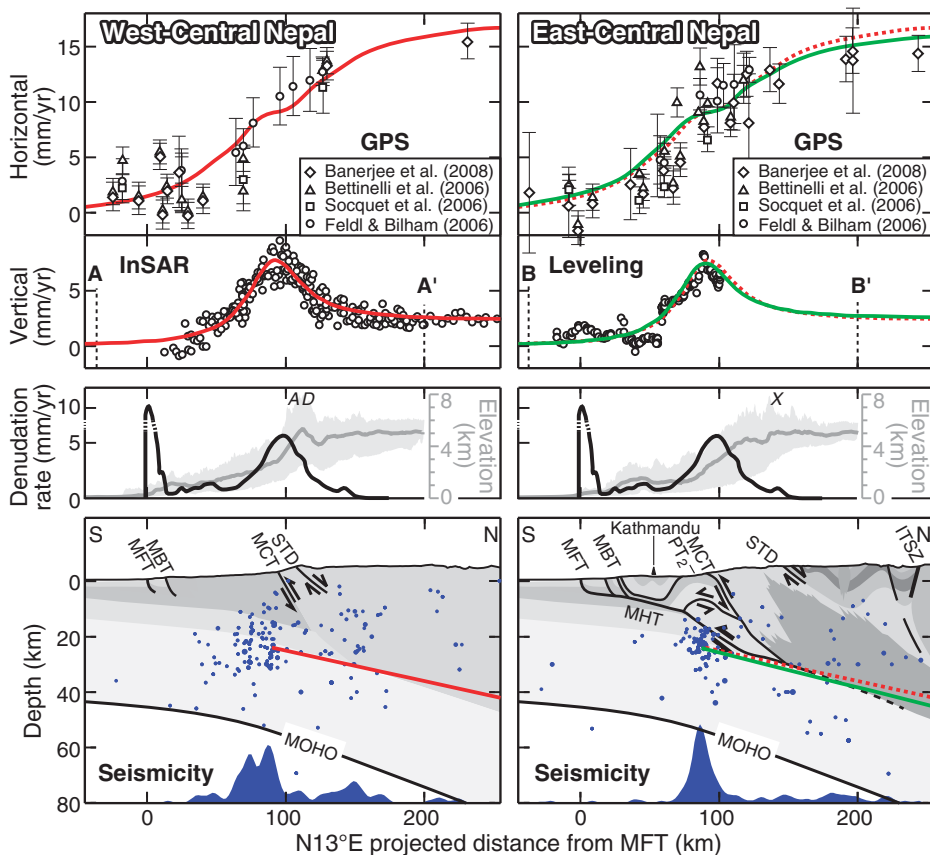


Figure 2. Geometry of the Main Himalayan Thrust (MHT). Upper panel: Profiles perpendicular to the mountain range in west-central (left) and east-central Nepal (right) showing the horizontal velocities derived from GPS and the vertical velocities derived from interferometric synthetic aperture radar (InSAR) and leveling. Geodetic data have been projected along the profiles indicated in Figure 1. Error bars denote 1σ uncertainties on GPS velocities. Uncertainties on leveling and InSAR are 0.2–2.8 mm/yr and 0.7–3.1 mm/yr, respectively. Colored curves correspond to modeled interseismic deformation using a buried-fault model. West-central Nepal (red): dip = 6.5° , depth = 24.1 km, slip rate = 20.6 mm/yr. East-central Nepal (green): dip = 7.4° , depth = 24.2 km, slip rate = 19.6 mm/yr. The modeled deformation in west-central Nepal has been duplicated on the right panel for comparison (dashed red line). Middle panel: Stack of six denudation profiles determined from a study of river incision (black line; Lavé and Avouac, 2001). Note that the same vertical scale is used to represent interseismic uplift and denudation rates. The average topographic profile is indicated in gray, with envelope showing minimum and maximum elevations in an ~ 100 -km-wide box centered on the main profiles. Lower panel: Geometry of the two inverted dislocations (red and green lines) represented on typical cross sections, showing main faults at depth (STD—South Tibetan Detachment; ITSZ—Indus Tsangpo Suture Zone) (Lavé and Avouac, 2001). Blue histogram shows distribution of seismic activity along the profile. Vertical exaggeration in lower panel is $2\times$.

topography to curb the impact of image distortion and limit geometrical decorrelation (Doin et al., 2011). A small-baseline strategy is implemented to take advantage of the redundancy on phase information and compensate for phase noise (Pinel-Puysségur et al., 2012). Digital elevation model (DEM) errors are determined by exploiting the proportionality between the perpendicular baseline and the local (wrapped) phase variability within the interferometric network (Ducret et al., 2011). Using independent atmospheric data provided by the ERA-Interim reanalysis of European Centre for Medium-Range Weather Forecasts (ECMWF), we further correct the interferograms from the contribution of stratified tropospheric delays (Jolivet

et al., 2011). Corrected interferograms are then filtered, unwrapped, and geocoded. The impact of atmospheric turbulence is reduced by the summation of 14 coherent interferograms, spanning a total period of observation of 45 yr in the final line-of-sight velocity map (Fig. 1). Due to the acquisition geometry, the resulting stack is insensitive to horizontal shortening across the Himalaya, and primarily includes the contribution of the vertical component of the deformation.

INTERSEISMIC UPLIFT ACROSS THE HIMALAYA

In the InSAR stack, we observe a band of uplifting terrain aligned with the trend of the

Himalaya, ~ 25 km south of the highest peaks. This uplift signal shows no correlation with surface elevation, indicating that the effect of tropospheric stratification has been correctly compensated. We reference the deformation with respect to a stable Tibetan Plateau, where no notable interseismic deformation is observed. The location (~ 100 km north of the MFT), amplitude (5–7 mm/yr), and spatial wavelength (50 km) of the peak uplift measured by InSAR are consistent with previous spirit leveling measurements in the Kathmandu area (east-central Nepal; see Fig. 1) (Bilham et al., 1997). In addition, a remarkable agreement between the location of the band of uplifting terrain imaged by InSAR and the microseismicity belt along the MHT is found (Pandey et al., 1995). Finally, the maximum gradient of interseismic horizontal shortening measured by GPS in central Nepal is co-located with the peak uplift detected with InSAR, in agreement with theoretical expectations (Bettinelli et al., 2006). Therefore, the geodetic data set combined here for the measurement of interseismic strain in Nepal (InSAR, leveling, and GPS) is internally consistent.

The simplest hypothesis on the cause of interseismic strain in Nepal is continuous aseismic creep on the deep portion of the MHT, while its shallow portion from the latitude of the High Himalaya to the MFT is locked (Fig. 2) (Vergne et al., 2001). Here, we model the creeping fault as a planar semi-infinite dislocation embedded in an elastic half-space (Okada, 1985), and we invert separately the geodetic data of east-central and west-central Nepal to infer possible lateral variations in the configuration of the MHT. Fault strike and rake are fixed to simulate a convergence direction of $N10^\circ E$ in west-central Nepal and $N05^\circ E$ in east-central Nepal, which accounts for the curvature of the plate boundary. Using a combination of horizontal (GPS) and vertical (InSAR or leveling) data, we invert for the depth of the top of the dislocation, its dip angle, and its slip rate using a nonlinear inversion method (Tarantola and Valette, 1982). The comparison of the inversion results shows that fault geometry and slip rate cannot be distinguished between east-central and west-central Nepal within the uncertainty of the data, suggesting that lateral variations of the properties of the MHT in central Nepal are small (Fig. 2). The preferred model indicates that interseismic deformation is induced by a fault dipping at 3° – 7° , buried at a depth of 20–24 km, with a slip rate of 18–21 mm/yr. This inferred deep creeping portion of the MHT appears to correspond with a seismically imaged low-velocity zone under southern Tibet (Nábělek et al., 2009). The updip projection of the modeled dislocation intersects the surface well to the south of the active trace of the MFT (see Fig. 2), suggesting that the MHT dips on average more steeply at seismogenic depth than at greater depth in the

stable-sliding domain. This is consistent with the flat-ramp-flat geometry of the underlying MHT that has been inferred from the long-recognized antiformal structure of the Lesser Himalaya (Fig. 2) (Schelling, 1992).

DISCUSSION

Current deformation measured by geodesy indicates that deep aseismic creep terminates at the bottom of the mid-crustal ramp, which is consistent with full locking of the ramp and frontal flat during the interseismic period. Great historical earthquakes are believed to be caused by rupture of this locked portion of the fault system, thereby compensating the deformation accumulated during the interseismic period. However, due to the nonplanar geometry of the MHT, permanent deformation is expected to remain after each seismic cycle, which should be manifested by a net uplift centered above the mid-crustal ramp. Therefore, if thrusting occurred over a mid-crustal ramp with a fixed geometry, an ~20 km north-south separation should be observed between the transient (interseismic, above the base of the ramp) and permanent (long-term, above the middle of the ramp) peaks of uplift (Cattin and Avouac, 2000) (Fig. 3A).

On the other hand, the study of trans-Himalayan river profiles provides constraints on the denudation processes that compete with this expected long-term uplift (Lavé and Avouac, 2001; Seeber and Gornitz, 1983; Meade, 2010). This independent geomorphological approach

indicates that the locus of maximum long-term uplift is actually situated at the same latitude as the interseismic uplift peak measured by geodesy from InSAR and leveling (Fig. 2).

This spatial correspondence conflicts with the prediction, but can be accounted for by several interpretations. Long-term and interseismic uplift could be collocated if coseismic deformation related to slip on the MFT were not sufficient to compensate for interseismic uplift (Bilham et al., 1997; Meade, 2010). Indeed, although geomorphological evidence above the MFT indicates that nearly all of the shortening between Tibet and India is accommodated at the front of the system, suggesting no or little convergence deficit on the MFT (Lavé and Avouac, 2001), it is difficult to rule out the possibility of a few mm/yr of permanent shortening in the High Himalaya. Thus, a recently proposed mechanism is the out-of-sequence activation of a new thrust fault intersecting the surface 0–35 km to the south of the mapped trace of the MCT, and outcropping near the break in topographic slope identified as a physiographic transition (PT₂) (Wobus et al., 2005) (Figs. 1 and 3B). However, our inversions show that the base of the locked portion of the MHT is located at a depth of ~20 km, between 0 km and 20 km to the north of PT₂ (Fig. 2). If a thrust fault connected PT₂ with the locking transition of the MHT, then the observed spatial matching between long-term and interseismic uplift would require an extremely high dip angle for this hypothesized fault (45°–90°). Such a steep

dip angle would be incompatible with theoretical constraints on reverse fault geometry provided by rock mechanics.

An alternative model of mountain building postulates that a strong topographic gradient within the overriding block may be created by accretion of material from the footwall to the hanging wall across the plate interface (Fig. 3C) (Robinson et al., 2003). Over several million years, numerical simulations of this underplating process assume a continuous flux of material across the mid-crustal ramp (Bollinger et al., 2006). However, on smaller time scales, accretion likely proceeds by discontinuous ramp jumps toward the foreland, leading to the formation of a crustal-scale duplex (Schelling, 1992). Migration of the ramp is expected to produce a gradual southward migration of the topographic front that would tend to be lessened by erosion. In the case of rapid erosion processes, a steady-state situation should emerge, where the peak of long-term uplift, which should roughly correspond to the location of the ramp, should be at any time located south of the peak of transient interseismic uplift (Burbank et al., 2003). Yet, the locus of maximum long-term denudation rate—which reflects the result of the competition between erosion processes and rock uplift—appears to be located to the north of the latitude of today's mid-crustal ramp inferred from our inversions, indicating that the system is out of equilibrium. Alternatively, the observed coincidence between the peak of interseismic uplift (marking the surface projection of the locked-to-unlocked transition on the MHT) and the peak of long-term uplift (marking the average position of the ramp over a period of time greatly exceeding the duration of a seismic cycle) could be compatible with delayed erosional response to a recent southward migration of the ramp. Assuming that a 20 km north-south offset between the two peaks is achieved when the geometry remains fixed (Cattin and Avouac, 2000), and if erosion operates on timescales of 0.1–1 m.y. (Lavé and Avouac, 2001), then the preservation of a coincidence between the two peaks requires an apparent ramp migration velocity of 20–200 mm/yr. This rate largely exceeds the average overthrusting rate of 5 mm/yr inferred from the thermal structure of the Nepal Himalaya for the past 10 m.y. (Bollinger et al., 2006; Herman et al., 2010). Therefore, our observations indicate that a southward jump of the mid-crustal ramp has taken place recently in central Nepal (83°E–86°E), adding support to the idea that underplating, which is capable of maintaining the steep topography of the High Himalaya on the long term, is a discontinuous process in time. Resolving potential lateral variations in the interseismic uplift pattern along the plate boundary is now required to understand how the segmentation of the MFT, which ultimately controls the size of great Himalayan

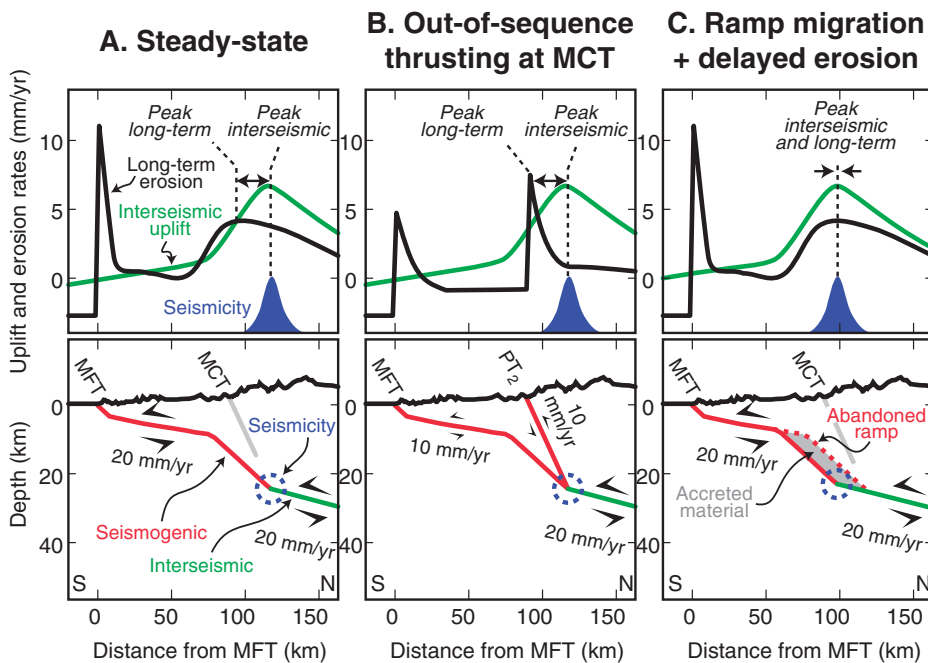


Figure 3. Seismic cycle, topographic construction, and long-term evolution of the Main Himalayan Thrust (MHT). Three models showing possible spatial relationship between interseismic uplift profile (green curve at top), long-term uplift profile (black curve at top), and microseismicity (blue histogram at top) as a function of the underlying processes taking place within the seismogenic crust.

earthquakes, could be related to the underlying long-term evolution of the MHT system.

CONCLUSIONS

Mountain growth in the Himalaya is to a large extent controlled by the presence of a mid-crustal ramp within the MHT system. Interseismic InSAR measurements indicate that the ramp is locked during the interseismic intervals, causing transient surface uplift above the transition zone. Over a large number of seismic cycles, the flat-ramp-flat shape of the plate interface is expected to induce permanent uplift above the ramp, whose surface expression is subdued by erosion, but which is responsible for prominent topographic slopes and steep river profiles across the High Himalaya. However, on the longer term, damage in the vicinity of the ramp produces occasional brittle failure within the Indian plate that may bypass the MHT and lead to an apparent southward migration of the mid-crustal ramp. Delayed erosional response to such episodes of frontward ramp jump can produce the observed coincidence between the peak of interseismic uplift detected by geodesy and the peak of permanent uplift deduced from riverbed morphology, which could not be otherwise explained by a steady-state model of mountain growth.

ACKNOWLEDGMENTS

ENVISAT data were provided through European Space Agency (ESA) program Dragon-2. The seismic catalog was provided by National Seismological Centre (NSC) of Nepal. Interferometric processing partly relies on the ROI_PAC software (Rosen et al., 2004). Postdoctoral fellowship for Grandin was provided by French Centre National d'Etudes Spatiales (CNES). We acknowledge funding from Institut National des Sciences de l'Univers (CT-Risk), ESA's Young Scientist Program, and Agence Nationale de la Recherche (ANR) via project EFIDIR (ANR-07-MDCO-004). This project was carried out within the frame of the joint ENS-CEA laboratory "LRC Yves Rocard". We thank reviewers Roger Bilham, Roland Bürgmann, Tim J. Wright, and Sandra J. Wyld for their useful comments.

REFERENCES CITED

- Banerjee, P., Bürgmann, R., Nagarajan, B., and Apel, E., 2008, Intraplate deformation of the Indian subcontinent: *Geophysical Research Letters*, v. 35, L18301, doi:10.1029/2008GL035468.
- Bettinelli, P., Avouac, J.-P., Flouzat, M., Jouanne, F., Bollinger, L., Willis, P., and Chitrakar, G.R., 2006, Plate motion of India and interseismic strain in the Nepal Himalaya from GPS and DORIS measurements: *Journal of Geodesy*, v. 80, p. 567–589, doi:10.1007/s00190-006-0030-3.
- Bilham, R., and 24 others, 1997, GPS measurements of present-day convergence across the Nepal Himalaya: *Nature*, v. 386, p. 61–64, doi:10.1038/386061a0.
- Bollinger, L., Henry, P., and Avouac, J.P., 2006, Mountain building in the Nepal Himalaya: Thermal and kinematic model: *Earth and Planetary Science Letters*, v. 244, p. 58–71, doi:10.1016/j.epsl.2006.01.045.
- Burbank, D.W., Blythe, A.E., Putkonen, J., Pratt-Sitaula, B., Gabet, E., Oskin, M., Barros, A., and Ojha, T.P., 2003, Decoupling of erosion and precipitation in the Himalayas: *Nature*, v. 426, p. 652–655, doi:10.1038/nature02187.
- Cattin, R., and Avouac, J.-P., 2000, Modeling mountain building and the seismic cycle in the Himalaya of Nepal: *Journal of Geophysical Research*, v. 105, p. 13,389–13,407, doi:10.1029/2000JB900032.
- Doin, M.-P., Guillaso, S., Jolivet, R., Lasserre, C., Lodge, F., Ducret, G., and Grandin, R., 2011, Presentation of the small-baseline NSBAS processing chain on a case example: The Etna deformation monitoring from 2003 to 2010 using ENVISAT data: *Proceedings of the European Space Agency Symposium "Fringe"*, Frascati, Italy, 19–23 September 2011, p. 303–304: http://earth.eo.esa.int/workshops/fringe2011/files/FRINGE2011_Abstracts_Book.pdf.
- Ducret, G., Doin, M.-P., Grandin, R., Lasserre, C., and Guillaso, S., 2011, DEM corrections before unwrapping in a small baseline strategy for InSAR time series analysis: *Proceedings of the IEEE International Geoscience and Remote Sensing Symposium*, Vancouver, Canada, 24–29 July 2011, p. 1353–1356: <http://www.ustream.tv/recorded/16259302> (May 2012).
- Feldl, N., and Bilham, R., 2006, Great Himalayan earthquakes and the Tibetan Plateau: *Nature*, v. 444, p. 165–170, doi:10.1038/nature05199.
- Herman, F., Copeland, P., Avouac, J.-P., Bollinger, L., Mahéo, G., Le Fort, P., Rai, S., Foster, D., Pécher, A., Stüwe, K., and Henry, P., 2010, Exhumation, crustal deformation, and thermal structure of the Nepal Himalaya derived from the inversion of thermochronological and thermobarometric data and modeling of the topography: *Journal of Geophysical Research*, v. 115, B06407, doi:10.1029/2008JB006126.
- Hodges, K.V., Wobus, C., Ruhl, K., Schildgen, T., and Whipple, K., 2004, Quaternary deformation, river steepening, and heavy precipitation at the front of the Higher Himalayan ranges: *Earth and Planetary Science Letters*, v. 220, p. 379–389, doi:10.1016/S0012-821X(04)00063-9.
- Jackson, M., and Bilham, R., 1994, Constraints on Himalayan deformation inferred from vertical velocity fields in Nepal and Tibet: *Journal of Geophysical Research*, v. 99, p. 13,897–13,912, doi:10.1029/94JB00714.
- Jolivet, R., Grandin, R., Lasserre, C., Doin, M.-P., and Peltzer, G., 2011, Systematic InSAR tropospheric phase delay corrections from global meteorological reanalysis data: *Geophysical Research Letters*, v. 38, L17311, doi:10.1029/2011GL048757.
- Lavé, J., and Avouac, J.P., 2001, Fluvial incision and tectonic uplift across the Himalayas of central Nepal: *Journal of Geophysical Research*, v. 106, p. 26,561–26,591, doi:10.1029/2001JB000359.
- Meade, B.J., 2010, The signature of an unbalanced earthquake cycle in Himalayan topography?: *Geology*, v. 38, p. 987–990, doi:10.1130/G31439.1.
- Nábělek, J., Hetényi, G., Vergne, J., Sapkota, S., Kafle, B., Jiang, M., Su, H., Chen, J., Huang, B.-S., and the Hi-CLIMB Team, 2009, Underplating in the Himalaya-Tibet collision zone revealed by the Hi-CLIMB experiment: *Science*, v. 325, p. 1371–1374, doi:10.1126/science.1167719.
- Okada, Y., 1985, Surface deformation due to shear and tensile faults in a half-space: *Bulletin of the Seismological Society of America*, v. 75, no. 4, p. 1135–1154.
- Pandey, M.R., Tandukar, R.P., Avouac, J.P., Lave, J., and Massot, J.P., 1995, Interseismic strain accumulation on the Himalayan crustal ramp (Nepal): *Geophysical Research Letters*, v. 22, p. 751–754, doi:10.1029/94GL02971.
- Pinel-Puysségur, B., Michel, R., and Avouac, J.-Ph., 2012, Multi-Link InSAR time series: Enhancement of a wrapped interferometric database: *IEEE Journal of Selected Topics in Applied Earth Observations and Remote Sensing*, v. 5, doi:10.1109/JSTARS.2012.2196758.
- Robinson, D.M., DeCelles, P.G., Garzzone, C.N., Pearson, O.N., Harrison, T.M., and Catlos, E.J., 2003, Kinematic model for the Main central thrust in Nepal: *Geology*, v. 31, p. 359–362, doi:10.1130/0091-7613(2003)031<0359:KMFTMC>2.0.CO;2.
- Rosen, P.A., Henley, S., Peltzer, G., and Simons, M., 2004, Updated repeat orbit interferometry package released: Eos (Transactions, American Geophysical Union), v. 85, p. 47.
- Schelling, D., 1992, The tectonostratigraphy and structure of the eastern Nepal Himalaya: *Tectonics*, v. 11, p. 925–943, doi:10.1029/92TC00213.
- Seeber, L., and Gornitz, V., 1983, River profiles along the Himalayan arc as indicators of active tectonics: *Tectonophysics*, v. 92, p. 335–367, doi:10.1016/0040-1951(83)90201-9.
- Socquet, A., Vigny, C., Chamot-Rooke, N., Simons, W., Rangin, C., and Ambrosius, B., 2006, India and Sunda plates motion and deformation along their boundary in Myanmar determined by GPS: *Journal of Geophysical Research*, v. 111, B05406, doi:10.1029/2005JB003877.
- Tarantola, A., and Valette, B., 1982, Generalized nonlinear inverse problems solved using the least squares criterion: *Reviews of Geophysics and Space Physics*, v. 20, p. 219–232, doi:10.1029/RG020i002p00219.
- Vergne, J., Cattin, R., and Avouac, J.P., 2001, On the use of dislocations to model interseismic strain and stress build-up at intracontinental thrust faults: *Geophysical Journal International*, v. 147, p. 155–162, doi:10.1046/j.1365-246X.2001.00524.x.
- Wobus, C., Heimsath, A., Whipple, K., and Hodges, K., 2005, Active out-of-sequence thrust faulting in the central Nepalese Himalaya: *Nature*, v. 434, p. 1008–1011, doi:10.1038/nature03499.

Manuscript received 21 December 2011
Revised manuscript received 3 May 2012
Manuscript accepted 18 May 2012

Printed in USA